

STRUCTURAL AND MECHANICAL CHARACTERIZATION OF SPARK PLASMA SINTERED TUNGSTEN

ČECH Jaroslav¹, HAUŠILD Petr¹, KOČMANOVÁ Lenka^{1,2}, MATĚJÍČEK Jiří²

¹*Czech Technical University in Prague, Faculty of Nuclear Sciences and Physical Engineering, Prague, Czech Republic, EU, cechjar2@fffi.cvut.cz*

²*Institute of Plasma Physics, Prague, Czech Republic, EU, jmatejic@ipp.cas.cz*

Abstract

The main objective of this paper is to describe the microstructure and mechanical properties of spark plasma sintered tungsten. The indentation tests, which are very advantageous because of their semi-nondestructive character and low requirements on the volume of investigated material, were carried out using Berkovich and spherical indenters. Indentation techniques with spherical indenters are less frequently used than those with sharp indenters but they offer variation of strain with the indentation depth and, therefore, they could be used for determination of stress-strain curves. Local stress-strain behavior obtained by this method showed good correspondence with the results of compression tests. Observation of the microstructure and the fracture surfaces helped to explain some phenomena which occurred during the mechanical testing.

Keywords: Tungsten, SPS, instrumented indentation, stress-strain curve

1. INTRODUCTION

Tungsten is a metal with physical and mechanical properties desired in many applications, including future fusion devices. Nevertheless, the high melting temperature and hardness make the fabrication of tungsten parts by conventional methods very difficult. One of the possibilities how to prepare small and precise tungsten parts is powder metallurgy. In recent years, spark plasma sintering has become a method which is more frequently used in tungsten preparation due to lower temperature and shorter sintering time than conventional methods such as hot isostatic pressing.

Subsequent mechanical and structural characterization of these parts is necessary. Besides classical mechanical tests (e.g., tensile, hardness, fracture toughness tests), the techniques of instrumented indentation, where the penetration depth of indenter h and applied force F are continuously measured, have become widespread. By choosing various indenter shapes, information about many different mechanical properties can be obtained. Thus, instrumented indentation tests could represent an important alternative to the classical mechanical tests.

The advantages of instrumented indentation tests are their nondestructive character and low demands on the volume of the material under investigation. Indentation tests are very advantageous and in some cases also irreplaceable for the investigation of mechanical properties of welds [1] or individual phases of the material [2]. The most frequently used techniques are the tests with Berkovich indenter which gives the information about instrumented hardness and Young's modulus. The techniques with spherical indenters provide more detailed description of elastic-plastic properties of the material. With increasing penetration depth, the shape of the spherical indenter causes the change of strain. Thus, it is possible to investigate the evolution of stress with strain and to obtain the flow curve. Although we can obtain the stress-strain curve in the whole elastic-plastic range, in reality this is very complicated and several problems have to be solved.

The flow curves obtained by the instrumented indentation tests usually have a different shape than the curves from tensile tests [3], but methods for determining the yield strength, strain hardening exponent and other mechanical characteristics do exist. At low loads, the deformations are elastic, and the Hertz theory can be

used to calculate the stress and strain. With increasing load, plastic deformation starts to evolve in the material under the indenter. When the plastic zone reaches the surface of the sample, the ratio of hardness and yield strength H / σ_y stabilizes at the value of approximately 3. This evolution has been investigated and described by many authors [4, 5, 6]. The methods which enable the determination of the flow curve in the whole elastic and plastic range are presented for example in [7] and [8].

Another important issue is the real shape of spherical indenter. Many studies show that the real shape of the indenter differs from its nominal shape [9, 10, 11]. The inaccuracies in the indenter shape can introduce systematic errors in the determined values of mechanical properties. Another important question for very low indentation depths is the geometry of real contact between the indenter and the sample surface, where the surface roughness plays an important role.

In the present study, the method of instrumented indentation was used to determine mechanical properties of spark plasma sintered tungsten. The yield strength values were compared with the data from compression tests. The microstructure and fracture behavior were also studied.

2. EXPERIMENTAL PROCEDURE

Tungsten sample was prepared by spark plasma sintering from a $\sim 2 \mu\text{m}$ powder (Osram Bruntál, Czech Republic) in an SPS 10-4 machine (Thermal Technology, Santa Rosa, USA). The sintering was carried out at 1800 °C and 70 MPa for 3 minutes in a graphite die under an inert atmosphere.

A sample for metallographic analysis was mechanically polished with abrasive papers and diamond pastes and finished with OPS suspension. The sample was chemically etched in the solution of nitric and hydrofluoric acid. Analysis was performed using light metallographic and scanning electron microscope.

Hardness and Young's modulus were measured by Berkovich indenter calibrated on fused silica sample according to the ISO 14577 standard [12]. Data were evaluated using the Oliver-Pharr method [13]. The indentations were carried out on Anton Paar CSM NHT nanoindentation instrument at the load range 10-500 mN. The indentation sequence consisted of loading (30 s), holding at maximum load (10 s), and unloading (30 s).

Indentation tests with the spherical indenter of nominal radius 20 μm were performed in order to determine the stress-strain curve. The method with loadings and partial unloadings (so called continuous multicycle) was used. Each indentation consisted of 20 cycles composed of loading to the maximum force (10 s), holding period (5 s), and unloading to 20 % of maximum force (10 s). The maximum applied force of each cycle progressively increased from 10 mN to 500 mN. Since the radius of the spherical indenter was not supposed to be ideal, the calibration of indenter area function A_p using the theoretical value of Young's modulus of tungsten $E = 400 \text{ GPa}$ [14] was performed according to the equation

$$A_p = \frac{\pi S^2}{4E_r^2}, \quad (1)$$

where S stands for contact stiffness and E_r is reduced modulus of the specimen and the indenter. For an increasing contact depth h_c , the real radius was then determined from the geometry of the system as

$$R = \frac{\frac{A_p}{\pi} + h_c^2}{2h_c}. \quad (2)$$

Representative stress σ_{repr} and representative strain ε_{repr} were computed according to Tabor formulae [4]

$$\sigma_{repr} = \frac{F}{C\pi a^2}, \quad \varepsilon_{repr} = 0.2 \frac{a}{R}, \quad (3)$$

where a is the contact radius and C stands for the constraint factor equal to 3.

Yield strength was determined by the approach used in automated ball indentation tests (ABIT) described in [7]. Yield strength was computed from the equation

$$\sigma_y = \beta_m A, \quad (4)$$

where β_m is a material constant same for a given group of materials. A is a fitting parameter of the equation

$$\frac{F}{d_t^2} = A \left(\frac{d_t}{2R} \right)^{m-2}, \quad (5)$$

where m is Meyer's coefficient and d_t is total indentation diameter at maximum load.

To avoid the problems with transition from elastic to plastic region and the errors arising from the uncertainty of geometry of contact at low penetration depths, the cycles with low maximum load were excluded from our analysis.

The indentation tests with partial unloadings with the spherical indenter of 2.5 mm in diameter were also performed up to load 2 kN. Compression tests, which served as the comparison for the values of yield strength determined by indentation, were performed on testing machine Inspekt 100 kN on specimens with a cross-section of 5 mm x 5 mm and a height of 8 mm. During these ABIT and compression tests, cracking occurred. The fracture surfaces were examined in SEM.

3. RESULTS

The microstructure of spark plasma sintered tungsten is shown in **Fig. 1a**. Inside individual particles, (sub)grains of submicron size can be observed. Between individual particles, some voids were observed which suggest that the sintering did not result in complete densification of the powder as it is typical of this type of material processing.

The imprint created by Berkovich indenter in the surface with partially revealed microstructure is shown in **Fig. 2**. Young's modulus and indentation hardness were measured for depths from 200 nm to 2200 nm. Young's modulus remained constant through the whole range of measurements at $E_{IT} = 409 \pm 14$ GPa (**Fig. 3**). On the other hand, hardness was not constant and it increased with decreasing contact depth. The most significant decrease was seen at the contact depths up to approximately 500 nm. For higher depths, the hardness tended to stabilize at about $H_{IT} = 5650$ MPa (**Fig. 3**).

The $F-h$ indentation curve obtained by indentation with spherical indenter for the single indentation and the indentation with partial unloadings is shown in **Fig. 4a**. As can be seen from this figure, partial unloadings were fully elastic and they did not change the shape of the final indentation curve compared with the single indentation. The representative stress-representative strain curve obtained from these tests using the already calibrated indenter is presented in **Fig. 4b**. Data in the strain range 2-9 % were obtained. The constant β_m , which is necessary for evaluation of yield strength, was set to $\beta_m = 0.2285$ according to [15]. With this value of β_m , the value of yield strength was $\sigma_y = 1357 \pm 95$ MPa.

Yield strength from the compression tests was $\sigma_y = 1333 \pm 17$ MPa. Nearly immediately after reaching the yield strength in compression tests, the specimens started to collapse. Thus, the properties in the plastic region of stress-strain curve could not be determined in this way. Brittle behavior of spark plasma sintered tungsten was confirmed by indentation tests with spherical indenter 2.5 mm in diameter which caused cracking

of the sample for loads higher than 1600 N. Fracture surfaces were examined in scanning electron microscope (**Fig. 1b**). The fracture occurred entirely by interparticle decohesion (see e.g. [16]).

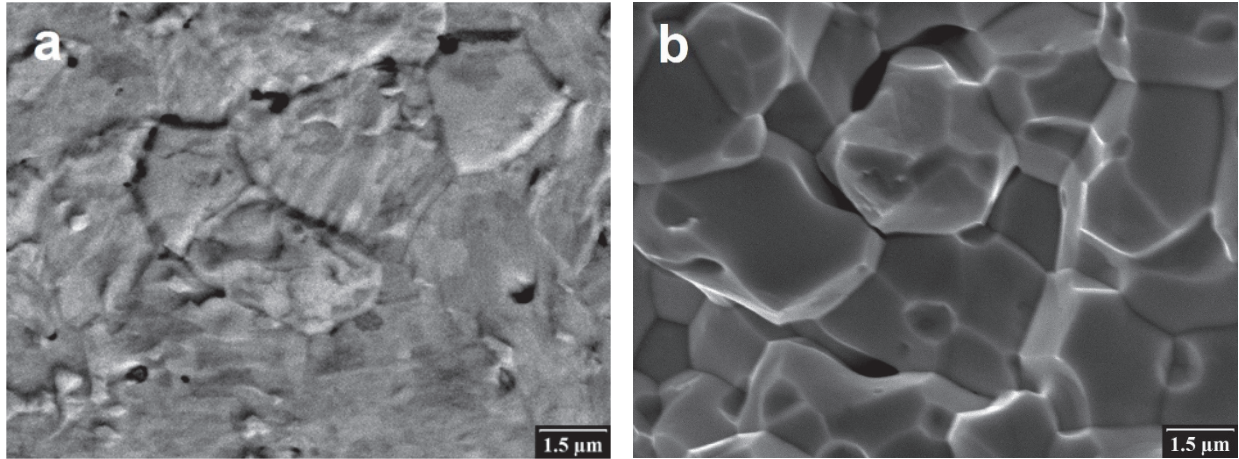


Fig. 1 (a) Microstructure and (b) fracture surface of SPS tungsten

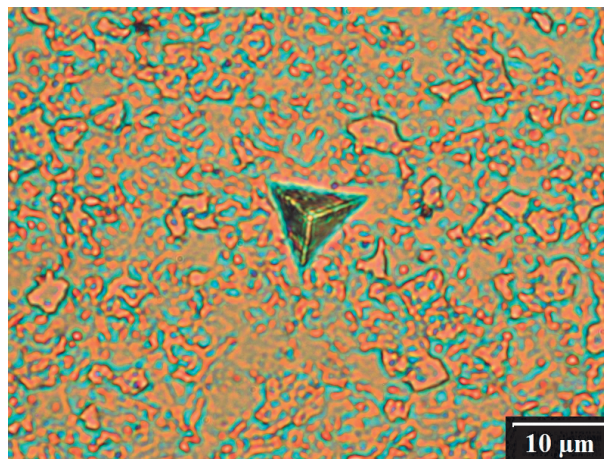


Fig. 2 Berkovich imprint on the surface with partially revealed microstructure

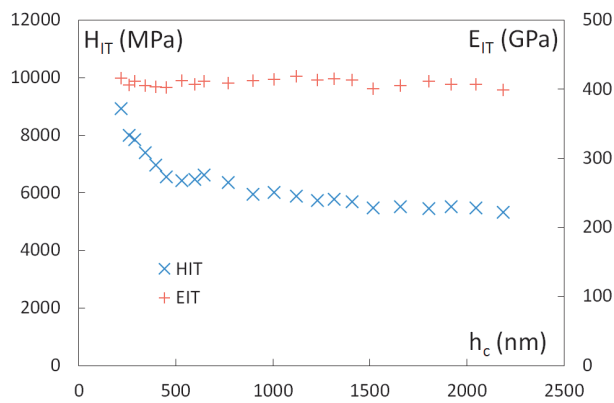


Fig. 3 Depth evolution of hardness of SPS tungsten

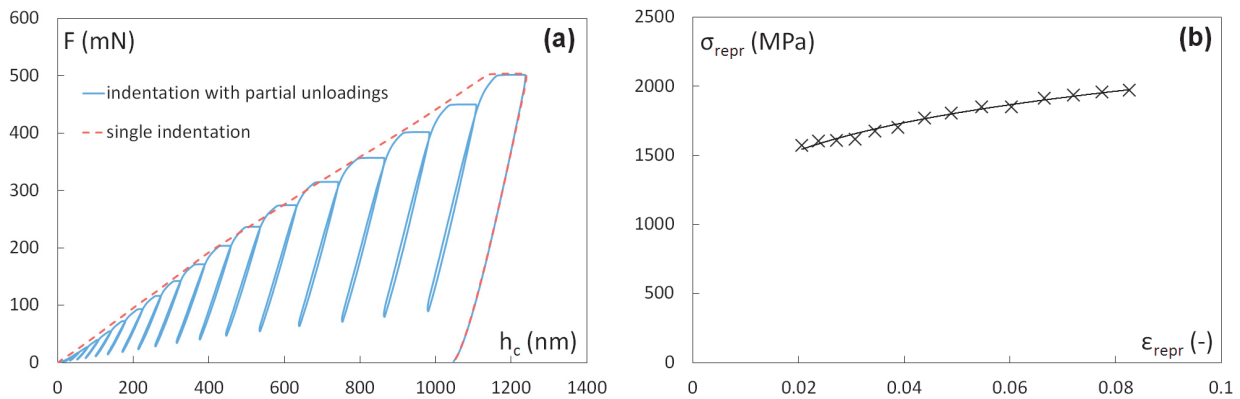


Fig. 4 (a) Typical indentation curves, (b) representative stress-strain curve

4. DISCUSSION

The results of Young's modulus measurements show that the nanoindentation technique with Berkovich indenter is well applicable for the determination of mechanical properties of spark plasma sintered tungsten. The constant value of Young's modulus with low scatter is in good agreement with the values of Young's modulus given in the literature [14].

The change in hardness observed with the increase in penetration depth could be caused by microstructural effects. As can be seen in Fig. 2, larger indents characterize the area corresponding to several powder particles including their bonding and also the voids between them. With decreasing size of indents, the microstructure of individual powder particles starts to play an important role. The presence of subgrains and the indentation size effect are the factors that can cause the increase in hardness with the decreasing size of indents.

Since the real radius of spherical indenter usually does not match the nominal value, calibration is necessary in order to obtain accurate stress-strain curves of any material [17]. Nevertheless, some type of input information is needed to calibrate the indenter. The most commonly used technique is based on the knowledge of Young's modulus. In this study, the literature value of Young's modulus $E = 400$ GPa is used; however, the theoretical value of Young's modulus is not known for every material. In that case, it is possible to use the value obtained by the indentation with Berkovich indenter which, in our case, meets well the theoretical values.

Moreover, if the indenter calibration and subsequent measurements are performed on the same material, the effect of pile-up can be eliminated. In this way, the effect of pile-up is already included in the calibration and no errors are introduced into the results as a consequence of this phenomenon.

The values of yield strength obtained by the instrumented indentation are in very good agreement with compression tests results.

Microstructure and fracture surface observations revealed numerous voids between original powder particles of spark plasma sintered tungsten. Moreover, the cracks propagated by the mechanism of interparticle decohesion. This indicates low cohesion of individual powder particles, which resulted in the brittle behavior observed during indentation and compression tests. The sintering process should therefore be optimized.

5. CONCLUSION

The structural and mechanical properties of spark plasma sintered tungsten were examined. The technique of instrumented indentation was successfully used to determine Young's modulus, hardness and stress-strain curves. Yield strength determined by spherical indenter is in very good agreement with the values from compression tests. Brittle behavior of this material, observed during indentation and compression tests, was

explained by the observation of voids and low cohesion of powder particles resulting in interparticle fracture. The results presented proved that the instrumented indentation is a suitable technique for mechanical characterization of the tungsten parts prepared by spark plasma sintering.

ACKNOWLEDGEMENTS

Support from Czech Technical University in Prague and from Technology Agency of the Czech Republic through grants no. SGS13/222/OHK4/3T/14 and TA03011266 is gratefully acknowledged.

REFERENCES

- [1] MURTY K.L., MIRAGLIA P.Q., MATHEW M.D., SHAH V.N., HAGGAG F.M. Characterization of gradients in mechanical properties of SA-533B steel welds using ball indentation. *International Journal of Pressure Vessels and Piping*, Vol. 76, No. 6, 1999, pp. 361-369.
- [2] ČECH J., HAUŠILD P., NOHAVA J., MATĚJÍČEK, J. Určování mechanických vlastností pomocí instrumentované indentace kulovým indentorem. In *JuveMatter 2014: Sborník přednášek studentské vědecké konference*. Praha: České vysoké učení technické v Praze, 2014, pp. 76-80.
- [3] HERBERT E.G., PHARR G.M., OLIVER W.C., LUCAS B.N., HAY J.L. On the measurement of stress-strain curves by spherical indentation. *Thin Solid Films*, Vol. 398-399, 2001, pp. 331-335.
- [4] TABOR D. *The Hardness of Metals*. Oxford University Press: London, 1951.
- [5] JOHNSON, K.L. *Contact Mechanics*. Cambridge University Press: Cambridge, 1985.
- [6] PARK Y.J., PHARR G.M. Nanoindentation with spherical indenters: Finite element studies of deformation in the elastic-plastic transition regime. *Thin Solid Films*, Vol. 447-448, 2004, pp. 246-250.
- [7] ASTM draft, standard test methods for automated ball indentation testing of metallic samples and structures to estimate stress-strain curves and ductility. 2007.
- [8] TALJAT B., ZACHARIA T., KOSEL F. New analytical procedure to determine stress-strain curve from spherical indentation data. *International Journal of Solids and Structures*, Vol. 35, No. 33, 1998, pp. 4411-4426.
- [9] FIELD J.S., SWAIN M.V. A simple predictive model for spherical indentation. *Journal of Materials Research*, Vol. 8, No. 2, 1993, pp. 297-306.
- [10] HERRMANN K., JENNETT N.M., WEGENER W., MENEVE J., HASCHKE K., SEEMANN R. Progress in determination of the area function of indenters used for nanoindentation. *Thin Solid Films*, Vol. 377-378, 2000, pp. 394-400.
- [11] HAUŠILD P., MATERNA A., NOHAVA J. On the identification of stress-strain relation by instrumented indentation with spherical indenter. *Materials and Design*, Vol. 37, No. 1, 2012, pp. 373-378.
- [12] ISO 14577, *Metallic materials - Instrumented indentation test for hardness and material parameters*. 2002.
- [13] OLIVER W.C., PHARR G.M. An improved technique for determining hardness and elastic modulus using load and displacement sensing indentation experiments. *Journal of Materials Research*, Vol. 7, No. 6, 1992, pp. 1564-1583.
- [14] *Metals Handbook, Vol.2 - Properties and Selection: Nonferrous Alloys and Special-Purpose Materials*. ASM International, 1990.
- [15] HAGGAG F.M., NANSTAD R.K., HUTTON J.T., THOMAS D.L., SWAIN R.L. Use of automated ball indentation to measure flow properties and estimate fracture toughness in metallic materials. In *Applications of Automation Technology to Fatigue and Fracture Testing*, ASTM 1092. Philadelphia: American Society for Testing and Materials, 1990, pp. 188-208.
- [16] SKIBA T., HAUŠILD P., KARLÍK M., VANMEENSEL K., VLEUGELS J. Mechanical properties of spark plasma sintered FeAl intermetallics. *Intermetallics*, Vol. 18, No. 7, 2010, pp. 1410-1414.
- [17] ČECH J., HAUŠILD P., NOHAVA J. Relation between indenter calibration and measured mechanical properties of elastic-plastic materials. In *Key Engineering Materials (Proceedings of 11th Conference on Local Mechanical Properties)*, in press.